

Contents lists available at ScienceDirect

Journal of Computational Physics

www.elsevier.com/locate/jcp



On some neural network architectures that can represent viscosity solutions of certain high dimensional Hamilton-Jacobi partial differential equations



Jérôme Darbon*, Tingwei Meng

Department of Applied Mathematics, Brown University, Providence, RI, 02912, USA

ARTICLE INFO

Article history: Received 4 March 2020 Received in revised form 30 September Accepted 1 October 2020

Keywords: equations

Available online 9 October 2020

Hamilton-Jacobi partial differential Neural networks Lax-Oleinik representation formula Grid-free numerical methods

ABSTRACT

We propose novel connections between several neural network architectures and viscosity solutions of some Hamilton-Jacobi (HJ) partial differential equations (PDEs) whose Hamiltonian is convex and only depends on the spatial gradient of the solution. To be specific, we prove that under certain assumptions, the two neural network architectures we proposed represent viscosity solutions to two sets of HJ PDEs with zero error. We also implement our proposed neural network architectures using Tensorflow and provide several examples and illustrations. Note that these neural network representations can avoid curve of dimensionality for certain HJ PDEs, since they do not involve neither grids nor discretization. Our results suggest that efficient dedicated hardware implementation for neural networks can be leveraged to evaluate viscosity solutions of certain HJ PDEs.

© 2020 Elsevier Inc. All rights reserved.

1. Introduction

Hamilton-Jacobi (HJ) partial differential equations (PDEs) arise in areas such as physics [1-5], optimal control [6-10], game theory [11-14], and imaging sciences [15-17]. In this paper, we consider HJ PDEs with state and time independent Hamiltonian function $H: \mathbb{R}^n \to \mathbb{R}$ and initial data $J: \mathbb{R}^n \to \mathbb{R}$ that read as follows

$$\begin{cases} \frac{\partial S}{\partial t}(\mathbf{x}, t) + H(\nabla_{\mathbf{x}} S(\mathbf{x}, t)) = 0 & \text{in } \mathbb{R}^n \times (0, +\infty), \\ S(\mathbf{x}, 0) = J(\mathbf{x}) & \text{in } \mathbb{R}^n. \end{cases}$$
(1)

The partial derivative with respect to t and the gradient vector with respect to \mathbf{x} of the solution $(\mathbf{x}, t) \mapsto S(\mathbf{x}, t)$ are denoted by $\frac{\partial S}{\partial t}(\mathbf{x},t)$ and $\nabla_{\mathbf{x}}S(\mathbf{x},t) = \left(\frac{\partial S}{\partial x_1}(\mathbf{x},t),\dots,\frac{\partial S}{\partial x_n}(\mathbf{x},t)\right)$, respectively. Note that the Hamiltonian H only depends on $\nabla_{\mathbf{x}}S(\mathbf{x},t)$. Recently, [18] establishes novel connections between some neural network architectures and the viscosity solution of a

set of HJ PDEs in the form of (1). (We refer readers to [6,19-21] for the definition of the viscosity solution.) In [18], the authors provided the conditions under which their proposed neural network architecture represents the viscosity solution to the corresponding HJ PDEs whose initial data J and Hamiltonian H are related to the parameters in the neural network. Note that in the HI PDEs they considered, the initial data I is assumed to be a convex piecewise affine function, and the Hamiltonian H also satisfies certain assumptions.

E-mail addresses: jerome_darbon@brown.edu (J. Darbon), tingwei_meng@brown.edu (T. Meng).

^{*} Corresponding author.

In this paper, we consider the HJ PDEs in the form of (1) satisfying other assumptions. For instance, the Hamiltonian H is convex, while the initial data J is not necessarily convex. Under these assumptions, we prove that the two neural network architectures depicted in Figs. 1 and 2 represent viscosity solutions to the corresponding HJ PDEs in the form of (1) with initial data J and convex Hamiltonian H. To be specific, in the first architecture shown in Fig. 1, the convex activation function L in the neural network gives the Lagrangian function, whose Fenchel-Legendre transform gives the Hamiltonian L in the corresponding HJ PDE. The initial data equals the minimum of several functions which are shifted copies of the asymptotic function L'_{∞} of L. The main result of this connection between the neural network architecture depicted in Fig. 1 and the corresponding HJ PDE is stated in Theorem 3.1. In the second architecture shown in Fig. 2, the activation function gives the initial data L in the HJ PDE. The Hamiltonian L is a piecewise affine convex function determined by the parameters in the neural network. The main result of this connection between the neural network architecture depicted in Fig. 2 and the corresponding HJ PDE is stated in Theorem 3.2.

To summarize, this paper investigates the connection between several neural network architectures and some specific sets of HJ PDEs. The motivations and advantages of this work are listed as follows

- Compared with traditional grid based representations, our proposed neural network representations do not involve any discretization of space and time. Hence these neural network representations can avoid the curse of dimensionality for certain HJ PDEs if the correct parameters are provided.
- Our novel connections between certain HJ PDEs and neural networks suggest a possible direction to solve some HJ PDEs by leveraging efficient hardware technologies and silicon-based electric circuits dedicated to neural networks. LeCun mentioned in [22] that the use of neural networks has been greatly influenced by available hardware. There have been many initiatives designing and constructing new hardware for extremely efficient (in terms of speed, latency, throughput or energy) implementations of neural networks. For instance, efficient neural network implementations are developed and optimized using field programmable gate arrays [23–25], Intel's architecture [26], Google's "Tensor Processor Unit" [27], and certain building blocks [28]. To obtain better performance on neural network computation, Xilinx announced a new set of hardware called Versal AI core, while Intel enhances their processors with specific hardware instructions. In addition, there is an evolution of silicon-based electrical circuits for machine learning, for which we refer readers to [29,30]. LeCun also suggests in [22, Sec. 3] possible new trends for hardware dedicated to neural networks. These trends for efficient neural network implementations motivate our study of the connections between neural network architectures and HJ PDEs.
- This work provides a possible interpretation of specific neural networks from the aspect of HJ PDEs.

Literature review. There is a huge body of literature on overcoming the curse of dimensionality of certain HJ PDEs. These works include, but are not limited to, max-plus algebra methods [10,31–38], dynamic programming and reinforcement learning [39,40], tensor decomposition techniques [41–43], sparse grids [44–46], model order reduction [47,48], polynomial approximation [49,50], optimization methods [15–17,51] and neural networks [18,52–62].

Recently, because of the trends for the efficient hardware implementations, neural networks have been increasingly applied in solving PDEs [52,53,55–96] and inverse problems involving PDEs [93,97–111]. Specifically, some high-dimensional HJ PDEs have been numerically solved using neural networks [18,55,57,62]. In [62], the solution to HJ PDEs is approximated by a deep neural network whose loss function is the l^2 error of the PDE, the initial condition and the boundary condition on randomly sampled points in the domain. In [55], a neural network architecture is proposed to approximate a backward stochastic differential equation which computes the solution to a second order HJ PDE via an associated stochastic representation formula. In [57], Huré $et\ al.$ approximate the solution and its gradient using two neural networks at each discretized time step. After the neural networks at a larger time t_{j+1} are trained, the neural networks at t_j are trained with loss function given by the error of the stochastic representation formula. In [18], a neural network architecture is proposed for representing the viscosity solution to certain high dimensional HJ PDEs without error. In addition, Cárdenas and Gibou [112] use neural networks to compute the mean curvature of the implicit level set function, which is the solution to a specific HJ PDE called level set equation.

Organization of this paper. This paper investigates the connections between two neural network architectures shown in Figs. 1 and 2 and the viscosity solution of some HJ PDEs whose initial data and Hamiltonian satisfy specific assumptions. In Sec. 2, we introduce basic concepts in finite dimensional convex analysis which will be used later in this paper. In Sec. 3, we present the main results. To be specific, we propose two neural network architectures. The first architecture is analyzed in Sec. 3.1, while the second one is analyzed in Sec. 3.2. Theorems 3.1 and 3.2 state that the neural network architectures shown in Figs. 1 and 2 represent viscosity solutions to the HJ PDEs with convex Hamiltonian *H* and initial data *J* satisfying certain assumptions. We provide several examples and illustrations after each theorem. Finally, a conclusion is drawn in Sec. 4.

2. Background

In this section, we introduce related concepts in convex analysis that will be used in this paper. We refer readers to Hiriart–Urruty and Lemaréchal [113,114] and Rockafellar [115] for comprehensive references on finite-dimensional convex

analysis. For the notation, we use \mathbb{R}^n to denote the *n*-dimensional Euclidean space, on which the Euclidean scalar product is denoted by $\langle \cdot, \cdot \rangle$.

Definition 1. (Convex sets and the unit simplex) A set $C \subset \mathbb{R}^n$ is called convex if for any $\lambda \in [0, 1]$ and any $\boldsymbol{x}, \boldsymbol{y} \in C$, the element $\lambda \boldsymbol{x} + (1 - \lambda) \boldsymbol{y}$ is in C. The unit simplex is a specific convex set in \mathbb{R}^n , denoted by Λ_n , defined by

$$\Lambda_n := \left\{ (\alpha_1, \dots, \alpha_n) \in [0, 1]^n : \sum_{i=1}^n \alpha_i = 1 \right\}.$$
 (2)

Definition 2. (Domains and proper functions) The domain of a function $f: \mathbb{R}^n \to \mathbb{R} \cup \{+\infty\}$ is the set

$$\operatorname{dom} f = \left\{ \boldsymbol{x} \in \mathbb{R}^n : f(\boldsymbol{x}) < +\infty \right\}.$$

A function $f: \mathbb{R}^n \to \mathbb{R} \cup \{+\infty\}$ is called proper if its domain is non-empty.

Definition 3. (Convex functions, concave functions and lower semicontinuity) A proper function $f: \mathbb{R}^n \to \mathbb{R} \cup \{+\infty\}$ is called convex if the set dom f is convex and if for any $\mathbf{x}, \mathbf{y} \in \text{dom } f$ and all $\lambda \in [0, 1]$, there holds

$$f(\lambda \mathbf{x} + (1 - \lambda)\mathbf{y}) \leq \lambda f(\mathbf{x}) + (1 - \lambda)f(\mathbf{y}).$$

A function $f: \mathbb{R}^n \to \mathbb{R} \cup \{-\infty\}$ is called concave if -f is a convex function. A proper function $f: \mathbb{R}^n \to \mathbb{R} \cup \{+\infty\}$ is called lower semicontinuous if for every sequence $\{\mathbf{x}_k\}_{k=1}^{+\infty}$ in \mathbb{R}^n with $\lim_{k \to +\infty} \mathbf{x}_k = \mathbf{x} \in \mathbb{R}^n$, we have $\liminf_{k \to +\infty} f(\mathbf{x}_k) \geqslant f(\mathbf{x})$. The class of proper, lower semicontinuous convex functions is denoted by $\Gamma_0(\mathbb{R}^n)$.

Definition 4. (Fenchel-Legendre transform) Let $f \in \Gamma_0(\mathbb{R}^n)$. The Fenchel-Legendre transform $f^* \colon \mathbb{R}^n \to \mathbb{R} \cup \{+\infty\}$ of f is defined as

$$f^*(\mathbf{p}) = \sup_{\mathbf{x} \in \mathbb{R}^n} \left\{ \langle \mathbf{p}, \mathbf{x} \rangle - f(\mathbf{x}) \right\}.$$

For any $f \in \Gamma_0(\mathbb{R}^n)$, the mapping $f \mapsto f^*$ is one-to-one. Moreover, there hold $f^* \in \Gamma_0(\mathbb{R}^n)$ and $(f^*)^* = f$.

Definition 5. (Inf-convolution) Let $f, g: \mathbb{R}^n \to \mathbb{R} \cup \{+\infty\}$ be two proper convex functions satisfying

$$f(\mathbf{x}) > \langle \mathbf{p}, \mathbf{x} \rangle + a$$
 and $g(\mathbf{x}) > \langle \mathbf{p}, \mathbf{x} \rangle + a$ for every $\mathbf{x} \in \mathbb{R}^n$, (3)

for some $\mathbf{p} \in \mathbb{R}^n$ and $a \in \mathbb{R}$. The inf-convolution of f and g, denoted by $f \square g$, is defined by

$$f \square g(\mathbf{x}) = \inf_{\mathbf{u} \in \mathbb{R}^n} \{ f(\mathbf{u}) + g(\mathbf{x} - \mathbf{u}) \}.$$

Moreover, the function $f \square g \colon \mathbb{R}^n \to \mathbb{R} \cup \{+\infty\}$ is a proper and convex function [113, Prop. IV.2.3.2].

Definition 6. (Asymptotic function) Let f be a function in $\Gamma_0(\mathbb{R}^n)$ and \mathbf{x}_0 be an arbitrary point in dom f. The asymptotic function of f, denoted by f'_{∞} , is defined by

$$f'_{\infty}(\mathbf{d}) = \sup_{s>0} \frac{f(\mathbf{x}_0 + s\mathbf{d}) - f(\mathbf{x}_0)}{s} = \lim_{s \to +\infty} \frac{f(\mathbf{x}_0 + s\mathbf{d}) - f(\mathbf{x}_0)}{s},\tag{4}$$

for every $\mathbf{d} \in \mathbb{R}^n$. In fact, this definition does not depend on the point \mathbf{x}_0 . Moreover, the asymptotic function f_{∞}' is convex and positive 1-homogeneous, i.e., $f_{\infty}'(\alpha \mathbf{d}) = \alpha f_{\infty}'(\mathbf{d})$ for every $\alpha > 0$ and $\mathbf{d} \in \mathbb{R}^n$. For details, see [113, Chap. IV.3.2]

We summarize some notations and definitions in Table 1.

3. Main results

In this paper, we consider the HI PDE given by

$$\begin{cases} \frac{\partial S}{\partial t}(\mathbf{x}, t) + H(\nabla_{\mathbf{x}} S(\mathbf{x}, t)) = 0 & \text{in } \mathbb{R}^n \times (0, +\infty), \\ S(\mathbf{x}, 0) = J(\mathbf{x}) & \text{in } \mathbb{R}^n, \end{cases}$$
(5)

where $H: \mathbb{R}^n \to \mathbb{R} \cup \{+\infty\}$ is called Hamiltonian, and $J: \mathbb{R}^n \to \mathbb{R}$ is the initial data. It is well-known that when H is convex, the viscosity solution is given by the Lax-Oleinik formula [19,116,117] stated as follows

Table 1 Notations used in this paper. Here, we use f, g to denote functions from \mathbb{R}^n to $\mathbb{R} \cup \{+\infty\}$ and $\mathbf{x}, \mathbf{y}, \mathbf{p}, \mathbf{d}$ to denote vectors in \mathbb{R}^n . For simplicity, we omit the assumptions in the definitions.

Notation	Meaning	Definition
$\langle \cdot, \cdot \rangle$	Euclidean scalar product in \mathbb{R}^n	$\langle \mathbf{x}, \mathbf{y} \rangle := \sum_{i=1}^{n} x_i y_i$
Λ_n	The unit simplex in \mathbb{R}^n	$\{(\alpha_1, \dots, \alpha_n) \in [0, 1]^n : \sum_{i=1}^n \alpha_i = 1\}$
dom f	The domain of f	$\{\mathbf{x} \in \mathbb{R}^n : f(\mathbf{x}) < +\infty\}$
$\Gamma_0(\mathbb{R}^n)$	A useful and standard class of convex functions	The set containing all proper, convex, lower semicontinuous functions from \mathbb{R}^n to
		$\mathbb{R} \cup \{+\infty\}$
f^*	Fenchel-Legendre transform of f	$f^*(\boldsymbol{p}) := \sup_{\boldsymbol{x} \in \mathbb{R}^n} \{ \langle \boldsymbol{p}, \boldsymbol{x} \rangle - f(\boldsymbol{x}) \}$
$f\square g$	Inf-convolution of f and g	$f \square g(\mathbf{x}) = \inf_{\mathbf{u} \in \mathbb{R}^n} \{ f(\mathbf{u}) + g(\mathbf{x} - \mathbf{u}) \}$
f_∞'	The asymptotic function of f	$f_{\infty}'(\boldsymbol{d}) = \sup_{s>0} \left\{ \frac{1}{s} (f(\boldsymbol{x}_0 + s\boldsymbol{d}) - f(\boldsymbol{x}_0)) \right\}$

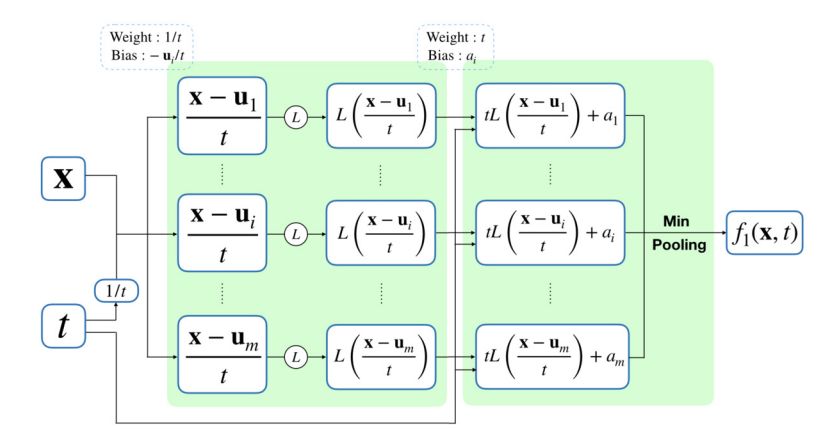


Fig. 1. An illustration of the architecture of the neural network (7) that represents the Lax-Oleinik formula with specific initial condition $J = f_1(\cdot, 0)$ defined in (10) and the convex Hamiltonian $H = L^*$.

$$S_{LO}(\mathbf{x},t) = \inf_{\mathbf{u} \in \mathbb{R}^n} \left\{ J(\mathbf{u}) + tH^* \left(\frac{\mathbf{x} - \mathbf{u}}{t} \right) \right\} = \inf_{\mathbf{v} \in \mathbb{R}^n} \left\{ J(\mathbf{x} - t\mathbf{v}) + tH^*(\mathbf{v}) \right\}, \tag{6}$$

where H^* is the Fenchel-Legendre transform of H.

In this part, we represent the Lax-Oleinik formula using two neural network architectures. The first one is given by

$$f_1(\mathbf{x},t) = \min_{i \in \{1,\dots,m\}} \left\{ tL\left(\frac{\mathbf{x} - \mathbf{u}_i}{t}\right) + a_i \right\}. \tag{7}$$

In this function, $\{(\boldsymbol{u}_i, a_i)\}_{i=1}^m \subset \mathbb{R}^n \times \mathbb{R}$ is the set of parameters, and the function $L \colon \mathbb{R}^n \to \mathbb{R}$ is the activation function, which corresponds to the Lagrangian function in the Hamilton–Jacobi theory. An illustration is shown in Fig. 1.

The second neural network architecture is defined by

$$f_2(\mathbf{x},t) = \min_{i \in \{1,\dots,m\}} \left\{ \tilde{J}(\mathbf{x} - t\mathbf{v}_i) + tb_i \right\}. \tag{8}$$

Here, $\{(\mathbf{v}_i, b_i)\}_{i=1}^m \subset \mathbb{R}^n \times \mathbb{R}$ is the set of parameters, and $\tilde{J} : \mathbb{R}^n \to \mathbb{R}$ is the activation function, which corresponds to the initial function in the HJ PDE. An illustration is shown in Fig. 2.

These two neural network architectures are further introduced and investigated in Section 3.1 and 3.2, respectively. To be specific, they are shown to represent a viscosity solution to certain HJ PDEs under some assumptions without errors. In addition, several examples are shown in each subsection. In these examples, certain HJ PDEs are solved using corresponding neural network architectures. The Tensorflow codes of these two neural networks using our proposed architectures are provided in the website https://github.com/TingweiMeng/NN_LO.

3.1. The first architecture

In this subsection, we analyze the first neural network architecture given by Eq. (7). Before introducing the main Theorem 3.1 in this subsection, we prove the following lemma which will be used in the proof of Theorem 3.1.

Lemma 3.1. Let f be a function in $\Gamma_0(\mathbb{R}^n)$ and f'_{∞} be the asymptotic function of f. Then, we have $f \Box f'_{\infty} = f$.

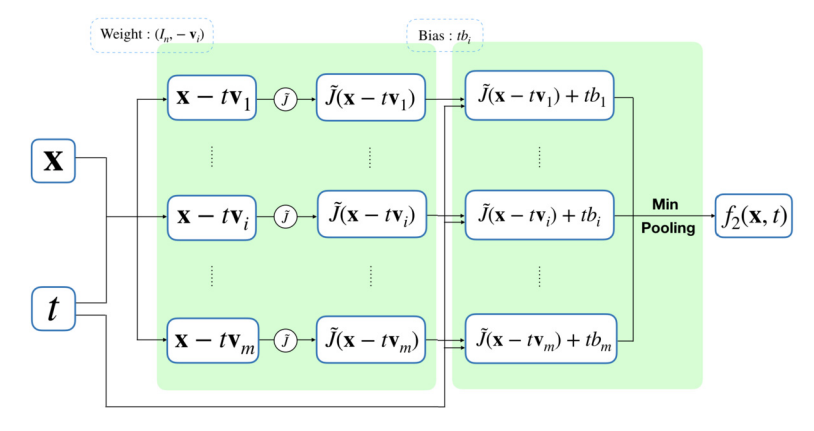


Fig. 2. An illustration of the architecture of the neural network (8) that represents the Lax-Oleinik formula with specific initial condition $J = \tilde{J}$ and the convex Hamiltonian H defined in (12).

Proof. First we consider the case when $x \in \text{dom } f$. By Definition 5 we have

$$(f\Box f'_{\infty})(\mathbf{x}) = \inf_{\mathbf{u} \in \mathbb{D}^n} \left\{ f(\mathbf{u}) + f'_{\infty}(\mathbf{x} - \mathbf{u}) \right\} \le f(\mathbf{x}) + f'_{\infty}(\mathbf{0}) = f(\mathbf{x}),$$

where the last equality holds because $f'_{\infty}(\mathbf{0}) = 0$ by Definition 6. On the other hand, taking s = 1, $\mathbf{d} = \mathbf{x} - \mathbf{u}$ and $\mathbf{x}_0 = \mathbf{u}$ in the second term in Eq. (4) in Definition 6, we obtain

$$f'_{\infty}(\mathbf{x} - \mathbf{u}) \ge f(\mathbf{u} + \mathbf{x} - \mathbf{u}) - f(\mathbf{u}) = f(\mathbf{x}) - f(\mathbf{u}), \tag{9}$$

for every $u \in \text{dom } f$. As a result, we have

$$(f\Box f_{\infty}')(\mathbf{x}) = \inf_{\mathbf{u} \in \text{dom } f} \left\{ f(\mathbf{u}) + f_{\infty}'(\mathbf{x} - \mathbf{u}) \right\} \ge \inf_{\mathbf{u} \in \text{dom } f} \left\{ f(\mathbf{u}) + f(\mathbf{x}) - f(\mathbf{u}) \right\} = f(\mathbf{x}).$$

Therefore, we conclude that $(f \Box f'_{\infty})(\mathbf{x}) = f(\mathbf{x})$ for every $\mathbf{x} \in \text{dom } f$.

Now we consider the case when $\mathbf{x} \notin \text{dom } f$ and prove $(f \Box f'_{\infty})(\mathbf{x}) = +\infty$. It suffices to prove $f'_{\infty}(\mathbf{x} - \mathbf{u}) = +\infty$ for all $\mathbf{u} \in \text{dom } f$. Since $\mathbf{u} \in \text{dom } f$, Eq. (9) still holds. As a result, we have

$$f'_{\infty}(\mathbf{x} - \mathbf{u}) > f(\mathbf{x}) - f(\mathbf{u}) = +\infty,$$

since $\mathbf{x} \notin \text{dom } f$ and $\mathbf{u} \in \text{dom } f$. Therefore, we conclude that $(f \Box f'_{\infty})(\mathbf{x}) = +\infty = f(\mathbf{x})$ for every $\mathbf{x} \notin \text{dom } f$. \Box

Now, we define the initial data $f_1(\cdot,0):\mathbb{R}^n\to\mathbb{R}$ as follows

$$f_1(\mathbf{x}, 0) = \min_{i \in \{1, \dots, m\}} \left\{ L'_{\infty}(\mathbf{x} - \mathbf{u}_i) + a_i \right\},\tag{10}$$

where L_{∞}' is the asymptotic function of L. Then, we present the main theorem stating that the function f_1 solves the HJ PDE (5) with the initial condition given by $J=f_1(\cdot,0)$ defined in (10) and the convex Hamiltonian H which is the Fenchel-Legendre transform of L.

Theorem 3.1. Let $L: \mathbb{R}^n \to \mathbb{R}$ be a convex uniformly Lipschitz function. Let f_1 be the function defined in (7). Then $f_1 = S_{L0}$, where S_{L0} is the Lax-Oleinik formula in (6) with the initial condition $J = f_1(\cdot, 0)$ defined in (10) and the convex Hamiltonian defined by $H = L^*$. Therefore, f_1 is a viscosity solution to the corresponding HJ PDE (5).

Remark 3.1. In the theorem above, we assume L to be a convex uniform Lipschitz function, which implies that its Fenchel–Legendre transform H has bounded domain, and hence H may take the value $+\infty$ somewhere. As a result, the uniqueness theorem of the viscosity solution in [116, Chap. 10.2] does not hold. To our knowledge, we are not aware of any uniqueness result of the viscosity solution to the HJ PDEs where dom H is bounded.

Proof. Since L is Lipschitz continuous, by [113, Prop. IV.3.2.7] L'_{∞} is finite valued, which implies that $\mathbb{R}^n \ni \mathbf{x} \mapsto f_1(\mathbf{x}, 0)$ is finite valued and it is a valid initial condition.

Let $\mathbf{x} \in \mathbb{R}^n$ and t > 0. By Definition 5 and (10), we have

$$S_{LO}(\mathbf{x}, t) = \inf_{\mathbf{u} \in \mathbb{R}^n} \left\{ J(\mathbf{u}) + tH^* \left(\frac{\mathbf{x} - \mathbf{u}}{t} \right) \right\} = \inf_{\mathbf{u} \in \mathbb{R}^n} \left\{ \min_{i \in \{1, \dots, m\}} \left\{ L'_{\infty}(\mathbf{u} - \mathbf{u}_i) + a_i \right\} + tH^* \left(\frac{\mathbf{x} - \mathbf{u}}{t} \right) \right\}$$

$$= \min_{i \in \{1, \dots, m\}} \left\{ a_i + \inf_{\mathbf{u} \in \mathbb{R}^n} \left\{ L'_{\infty}(\mathbf{u} - \mathbf{u}_i) + tH^* \left(\frac{\mathbf{x} - \mathbf{u}}{t} \right) \right\} \right\}$$

$$= \min_{i \in \{1, \dots, m\}} \left\{ a_i + \left(L'_{\infty} \Box tH^* \left(\frac{\cdot}{t} \right) \right) (\mathbf{x} - \mathbf{u}_i) \right\}.$$
(11)

Since L is convex with dom $L=\mathbb{R}^n$, then the function L is continuous [113, Thm. IV.3.1.2]. As a result, L is a function in $\Gamma_0(\mathbb{R}^n)$, hence we have $L=(L^*)^*$, which equals H^* because we assume $H=L^*$. Let t>0 and $h:\mathbb{R}^n\to\mathbb{R}$ be defined by $h(\mathbf{x})=tH^*\left(\frac{\mathbf{x}}{t}\right)=tL\left(\frac{\mathbf{x}}{t}\right)$ for every $\mathbf{x}\in\mathbb{R}^n$. Let \mathbf{x}_0 be an arbitrary point in dom h, which implies $\frac{\mathbf{x}_0}{t}\in\mathrm{dom}\ L$. By Definition 6, the asymptotic function of h evaluated at \mathbf{d} is given by

$$h'_{\infty}(\mathbf{d}) = \sup_{s>0} \left\{ \frac{1}{s} \left(tL\left(\frac{\mathbf{x}_0 + s\mathbf{d}}{t}\right) - tL\left(\frac{\mathbf{x}_0}{t}\right) \right) \right\} = \sup_{s>0} \left\{ \frac{t}{s} \left(L\left(\frac{\mathbf{x}_0}{t} + \frac{s}{t}\mathbf{d}\right) - L\left(\frac{\mathbf{x}_0}{t}\right) \right) \right\}$$
$$= \sup_{\tau>0} \left\{ \frac{1}{\tau} \left(L\left(\frac{\mathbf{x}_0}{t} + \tau\mathbf{d}\right) - L\left(\frac{\mathbf{x}_0}{t}\right) \right) \right\} = L'_{\infty}(\mathbf{d}),$$

where in the third equality we set $\tau = \frac{s}{t}$. Hence, using the equality above, the definition of h and by invoking Lemma 3.1, we obtain

$$\left(L_{\infty}'\Box tH^*\left(\frac{\cdot}{t}\right)\right)(\mathbf{x}-\mathbf{u}_i) = \left(h_{\infty}'\Box h\right)(\mathbf{x}-\mathbf{u}_i) = h(\mathbf{x}-\mathbf{u}_i) = tL\left(\frac{\mathbf{x}-\mathbf{u}_i}{t}\right).$$

We combine the equality above with (11), to obtain

$$S_{LO}(\boldsymbol{x},t) = \min_{i \in \{1,\dots,m\}} \left\{ a_i + \left(L_{\infty}' \Box t H^* \left(\frac{\cdot}{t} \right) \right) (\boldsymbol{x} - \boldsymbol{u}_i) \right\} = \min_{i \in \{1,\dots,m\}} \left\{ a_i + t L \left(\frac{\boldsymbol{x} - \boldsymbol{u}_i}{t} \right) \right\} = f_1(\boldsymbol{x},t).$$

Therefore, we conclude that $S_{L0}(\mathbf{x},t) = f_1(\mathbf{x},t)$ for each $\mathbf{x} \in \mathbb{R}^n$ and t > 0. Then, using the same proof as in [116, Sec. 10.3.4, Thm. 3], we conclude that f_1 is a viscosity solution to the corresponding HJ PDE (5). \Box

Remark 3.2. Although the initial conditions for the HJ PDE considered in Theorem 3.1 are given by a representation formula (10), it is not as restricted as it may seem to be. Indeed, the functions in the form of (10) can approximate a meaningful initial condition when m approaches infinity. We will illustrate this point using an example. Consider the Lagrangian function $L: \mathbb{R}^n \to \mathbb{R}$ satisfying $L'_{\infty} = \|\cdot\|$ (for instance when $L = \|\cdot\|$). Then the domain of the Hamiltonian H is the unit ball in \mathbb{R}^n , denoted by $B_1(\mathbb{R}^n)$. For this Hamiltonian, the reasonable set of initial data J is the set of 1-Lipschitz functions. From the physics point of view, the initial momentum p_0 (given by the gradient of J at the initial position \mathbf{x}_0) needs to be in dom $H = B_1(\mathbb{R}^n)$, in order to have a finite energy $H(\mathbf{p}_0)$. Therefore, the initial data J needs to be 1-Lipschitz. Now we argue that any 1-Lipschitz function can be approximated using functions in the form of (10) when m increases to infinity. As a result, any reasonable initial condition can be approximated using (10). Let $g: \mathbb{R}^n \to \mathbb{R}$ be an arbitrary 1-Lipschitz function. Let $\{\mathbf{u}_i\}$ be a dense sequence in \mathbb{R}^n and let $a_i:=g(\mathbf{u}_i)$ for each $i\in\{1,2,\ldots\}$. Define $g_m: \mathbb{R}^n \to \mathbb{R}$ by the formula in (10) with the chosen parameters $\{\mathbf{u}_i, a_i\}_{i=1}^m$, i.e., define g_m by

$$g_m(\mathbf{x}) := \min_{i \in \{1, \dots, m\}} \{ \|\mathbf{x} - \mathbf{u}_i\| + a_i \} = \min_{i \in \{1, \dots, m\}} \{ \|\mathbf{x} - \mathbf{u}_i\| + g(\mathbf{u}_i) \}.$$

It is straightforward to check that $g_m(\boldsymbol{u}_i) = g(\boldsymbol{u}_i)$ for each $i \in \{1, \dots, m\}$, and $g_m(\boldsymbol{x}) \geq g(\boldsymbol{x})$ for each $\boldsymbol{x} \in \mathbb{R}^n$, by using assumption that g is 1-Lipschitz. Therefore, $\{g_m\}$ is a decreasing sequence which is bounded below by g. Then, it is straightforward to check that g_m converges to g pointwisely as m going to infinity, by using the assumption that $\{\boldsymbol{u}_i\}$ is dense in \mathbb{R}^n and $\{g_m\}$, g are 1-Lipschitz. Moreover, this convergence can be improved to Γ -convergence, since we have the monotonicity $g_1 \geq g_2 \geq \cdots \geq g$. Therefore, in this example, the set of the functions in the form of (10) is actually dense (in the sense of pointwise convergence and Γ -convergence) in the set of 1-Lipschitz functions, which is a reasonable set for the initial conditions to the HJ PDEs with this Lagrangian L, as we claimed above.

Example 3.1. Let us consider the following one dimensional example that illustrates the function $f_1: \mathbb{R} \times [0, +\infty) \to \mathbb{R}$ with three neurons, i.e., we set n=1 and m=3. The Lagrangian L is defined as follows

$$L(x) = \begin{cases} -x - \frac{1}{2} & x < -1, \\ \frac{x^2}{2} & -1 \le x \le 2, \\ 2x - 2 & x > 2, \end{cases}$$

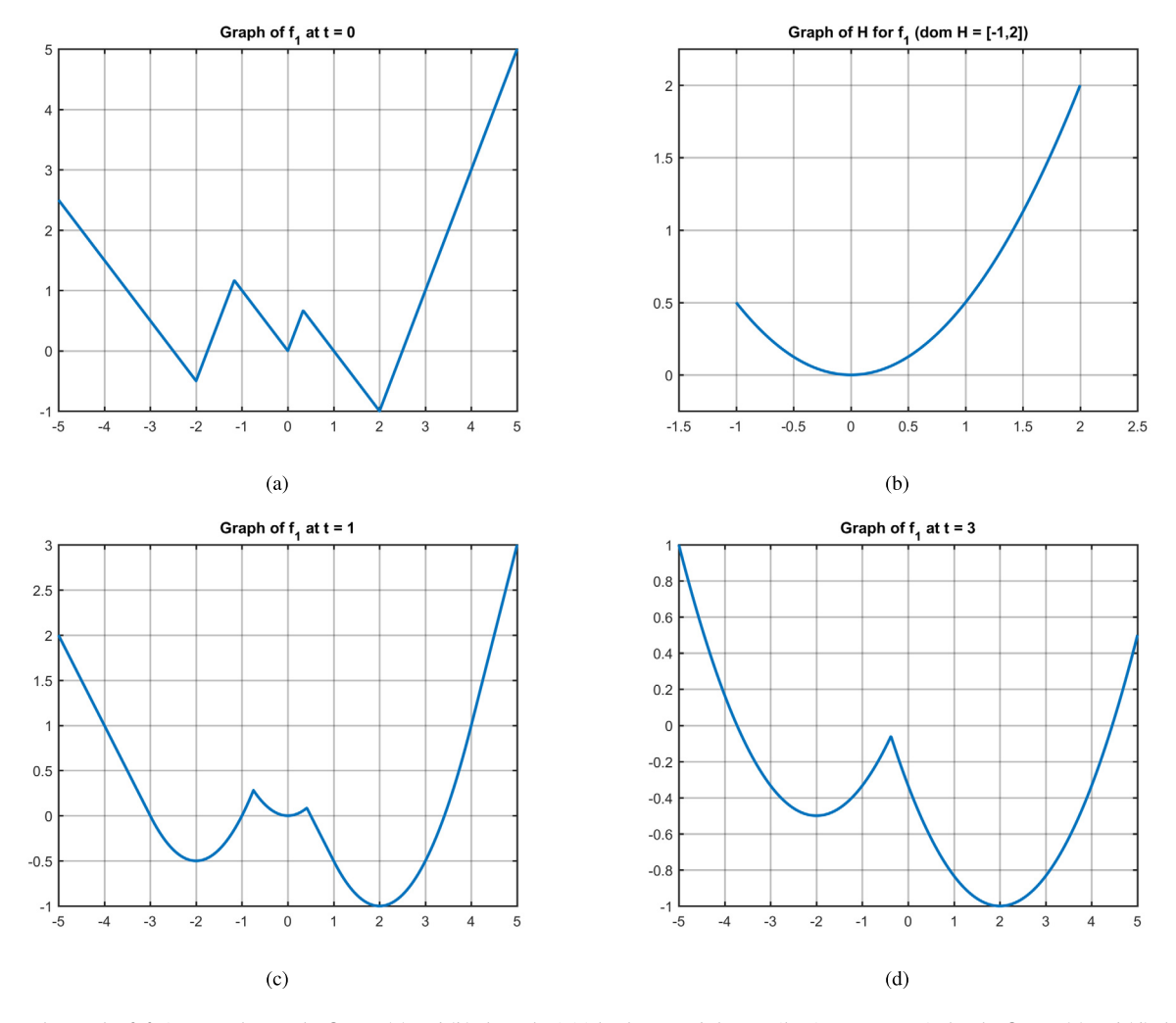


Fig. 3. The graph of f_1 in Example 3.1. The figures (a) and (b) show the initial value J and the Hamiltonian H, respectively. The figures (c) and (d) show the solution $S = f_1$ evaluated at t = 1 and t = 3, respectively.

for each $x \in \mathbb{R}$. Then, by Theorem 3.1, the Hamiltonian H is given by

$$H(p) = L^*(p) = \begin{cases} \frac{p^2}{2} & -1 \le p \le 2, \\ +\infty & \text{otherwise.} \end{cases}$$

Also, by Theorem 3.1, the initial data J is given by $f_1(\cdot,0)$ defined in (10). In other words, J is the minimum of three functions, each of which is a shift of the function L'_{∞} , which by Definition 6 reads as follows

$$L'_{\infty}(x) = \begin{cases} -x & x < 0, \\ 2x & x \ge 0. \end{cases}$$

In this example, we choose the parameters $(u_1, a_1) = (-2, -0.5)$, $(u_2, a_2) = (0, 0)$ and $(u_3, a_3) = (2, -1)$. The corresponding functions J, H and f_1 are shown in Fig. 3, where (a) shows the initial value J, (b) shows the convex Hamiltonian H, and (c) and (d) show the solution $S = f_1$ evaluated at t = 1 and t = 3, respectively. Note that our proposed architecture computes the viscosity solution without numerical errors. The viscosity solution in this example is not a classical solution, and there exist points where the solution is not differentiable. In Fig. 3 (c) and (d), we can observe kinks in the graph of the functions given by our proposed neural network architecture. It can be seen from the non-smoothness of the graphs in Fig. 3 (c) and (d) that our proposed architecture computes the viscosity solution without any numerical smoothing effect.

Example 3.2. We now present a high dimensional example. To be specific, the dimension is set to be n = 10, and the solution $f_1 : \mathbb{R}^{10} \times [0, +\infty) \to \mathbb{R}$ is represented by a neural network with three neurons, i.e., m = 3. The activation function L is given by

$$L(\mathbf{x}) = \max\{\|\mathbf{x}\|_2 - 1, 0\} = \begin{cases} \|\mathbf{x}\|_2 - 1 & \text{if } \|\mathbf{x}\|_2 > 1, \\ 0 & \text{if } \|\mathbf{x}\|_2 \le 1. \end{cases}$$

The corresponding Hamiltonian is given by

$$H(\boldsymbol{p}) = L^*(\boldsymbol{p}) = \begin{cases} \|\boldsymbol{p}\|_2 & \text{if } \|\boldsymbol{p}\|_2 \le 1, \\ +\infty & \text{if } \|\boldsymbol{p}\|_2 > 1. \end{cases}$$

The parameters are chosen to be $\mathbf{u}_1 = (-2, 0, 0, 0, \dots, 0)$, $\mathbf{u}_2 = (2, -2, -1, 0, \dots, 0)$, $\mathbf{u}_3 = (0, 2, 0, 0, \dots, 0)$, $a_1 = -0.5$, $a_2 = 0$ and $a_3 = -1$.

By Definition 6 and straightforward computation, we obtain $L'_{\infty}(\boldsymbol{d}) = \|\boldsymbol{d}\|_2$. Hence, the initial condition for the corresponding HJ PDE is given by Eq. (10), which in this example reads

$$J(\mathbf{x}) = \min_{i \in \{1,2,3\}} \{ \|\mathbf{x} - \mathbf{u}_i\|_2 + a_i \}.$$

The accompanying Fig. 4 shows the graph of f_1 for a 2-dimensional slice. To be specific, we fix $\mathbf{x} = (x_1, x_2, 0, \dots, 0)$, and compute $f_1(\mathbf{x}, t)$ at $t = 10^{-6}$, 1, 3 and 5. Note that the formula (7) is not well-defined for t = 0, hence we use a small number 10^{-6} instead. In each figure, the color is given by the function value $f_1(\mathbf{x}, t)$ and the x and y axes represent the variables x_1 and x_2 , respectively. The solutions evaluated at $t = 10^{-6}$, t = 1, t = 3 and t = 5 are shown in (a), (b), (c) and (d), respectively. The viscosity solution in this example is not a classical solution. Note that there are several kinks on some level curves of the solution in each figure in Fig. 4. Recall that the non-smoothness of the level curves implies the non-smoothness of the function. It can be seen from the non-smoothness of the level curves in Fig. 4 that our proposed architecture computes the viscosity solution without any numerical smoothing effect.

3.2. The second architecture

In this part, we analyze the second neural network architecture given by Eq. (8). Here, we assume the parameters $\{(\mathbf{v}_i, b_i)\}_{i=1}^m$ satisfy the following assumption

(H) There exists a convex function $\ell \colon \mathbb{R}^n \to \mathbb{R}$ satisfying $\ell(\mathbf{v}_i) = b_i$ for all $i \in \{1, \dots, m\}$.

Under this assumption, we present the following main theorem which states that the second architecture gives a viscosity solution to the corresponding HJ PDE, where the initial data is given by the activation function \tilde{J} in the neural network, and the Hamiltonian is a convex piecewise affine function determined by the parameters $\{(v_i, b_i)\}_{i=1}^m$.

Theorem 3.2. Assume the function $\tilde{J}: \mathbb{R}^n \to \mathbb{R}$ is a concave function and the assumption (H) is satisfied. Let f_2 be the function defined in (8). Then $f_2 = S_{LO}$, where S_{LO} is the Lax–Oleinik formula defined by (6) with initial condition $J = \tilde{J}$ and the Hamiltonian H defined by

$$H(\mathbf{p}) = \max_{i \in \{1, \dots, m\}} \left\{ \langle \mathbf{p}, \mathbf{v}_i \rangle - b_i \right\},\tag{12}$$

for every $\mathbf{p} \in \mathbb{R}^n$. Hence f_2 is a concave viscosity solution to the corresponding HJ PDE (5).

Proof. By assumption (H) and simply changing the notations in [18, Lem. 3.1], we have

$$H^*(\mathbf{v}) = \min \left\{ \sum_{i=1}^m \alpha_i b_i \colon (\alpha_1, \dots, \alpha_m) \in \Lambda_m, \sum_{i=1}^m \alpha_i \mathbf{v}_i = \mathbf{v} \right\},\tag{13}$$

for each $\mathbf{v} \in \text{co } \{\mathbf{v}_1, \dots, \mathbf{v}_m\} = \text{dom } H^*$, where Λ_m is the unit simplex defined in (2). Also, we have $H^*(\mathbf{v}_k) = b_k$ for each $k \in \{1, \dots, m\}$.

For each $\mathbf{x} \in \mathbb{R}^n$, t > 0 and $\mathbf{v} \in \operatorname{co} \{\mathbf{v}_1, \dots, \mathbf{v}_m\}$, let $\mathbf{\alpha} = (\alpha_1, \dots, \alpha_m) \in \Lambda_m$ be the minimizer in the minimization problem in (13) evaluated at \mathbf{v} . In other words, we have

$$\sum_{i=1}^{m} \alpha_i = 1, \quad \sum_{i=1}^{m} \alpha_i \mathbf{v}_i = \mathbf{v}, \quad \sum_{i=1}^{m} \alpha_i b_i = H^*(\mathbf{v}), \quad \text{and } \alpha_j \in [0, 1] \text{ for each } j \in \{1, \dots, m\}.$$

$$(14)$$

Then, by (14) and the assumption that $J = \tilde{J}$ is concave, we have

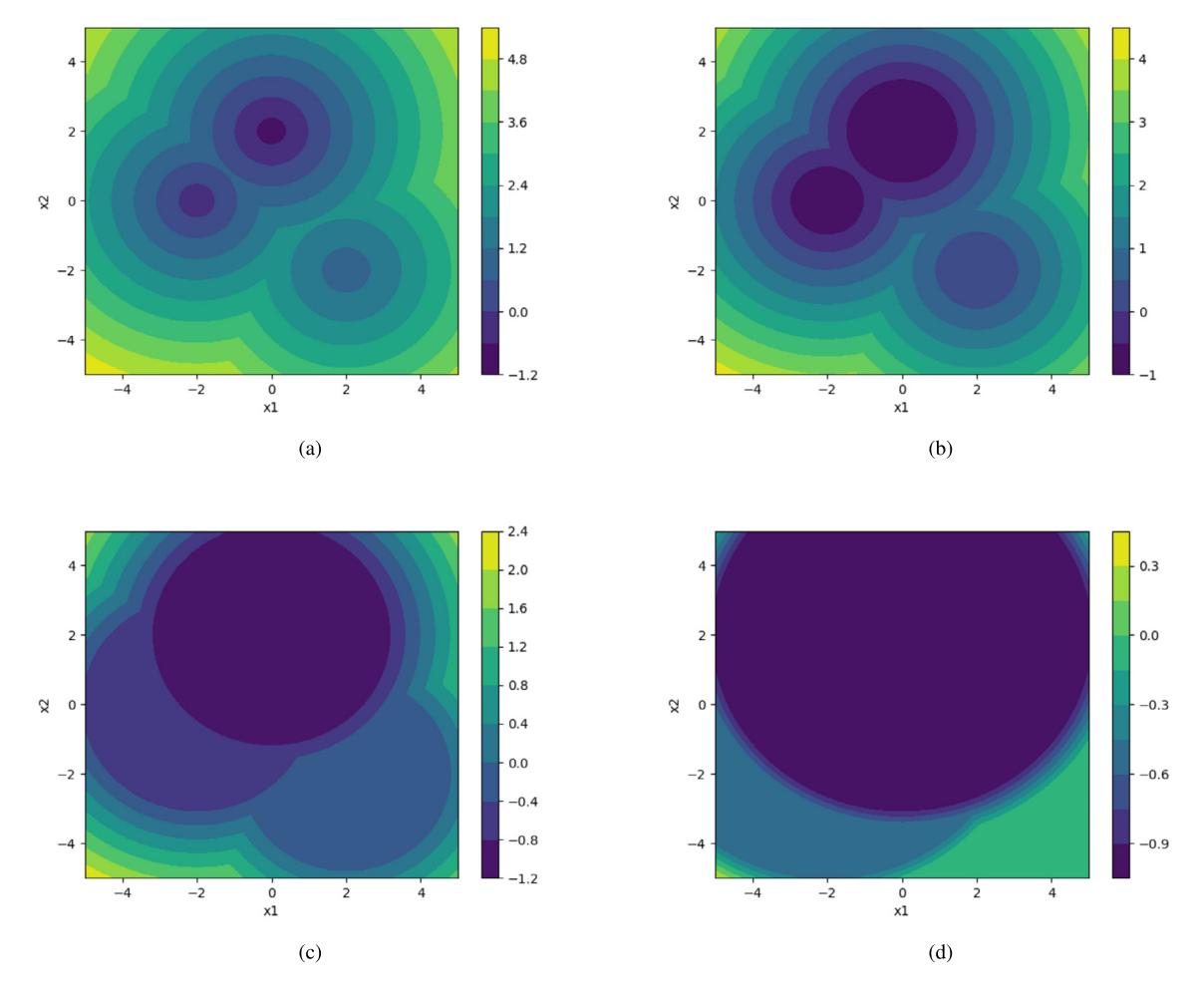


Fig. 4. A two dimensional slice of the graph of f_1 in Example 3.2. In each figure, the x and y axes correspond to the variables x_1 and x_2 , which are the first and second coordinates of the variable $\mathbf{x} = (x_1, x_2, 0, \dots, 0)$. The color is given by the function value $f_1(\mathbf{x}, t)$. The figures (a), (b), (c) and (d) show contour lines of the solution $f_1(\mathbf{x}, t)$ at $t = 10^{-6}$, t = 1, t = 3 and t = 5, respectively. (For interpretation of the colors in the figure(s), the reader is referred to the web version of this article.)

$$J(\boldsymbol{x} - t\boldsymbol{v}) + tH^*(\boldsymbol{v}) = J\left(\sum_{i=1}^{m} \alpha_i (\boldsymbol{x} - t\boldsymbol{v}_i)\right) + t\sum_{i=1}^{m} \alpha_i b_i \ge \sum_{i=1}^{m} \alpha_i J(\boldsymbol{x} - t\boldsymbol{v}_i) + \sum_{i=1}^{m} \alpha_i tb_i$$

$$= \sum_{i=1}^{m} \alpha_i (J(\boldsymbol{x} - t\boldsymbol{v}_i) + tb_i) \ge \min_{i \in \{1, \dots, m\}} \{J(\boldsymbol{x} - t\boldsymbol{v}_i) + tb_i\} = f_2(\boldsymbol{x}, t).$$

As a result, we conclude that

$$S_{LO}(\boldsymbol{x},t) = \inf_{\boldsymbol{v} \in \text{dom } H^*} \left\{ J(\boldsymbol{x} - t\boldsymbol{v}) + tH^*(\boldsymbol{v}) \right\} \geq f_2(\boldsymbol{x},t).$$

On the other hand, recall that $b_k = H^*(\mathbf{v}_k)$ for each $k \in \{1, ..., m\}$, hence we obtain

$$f_2(\boldsymbol{x},t) = \min_{i \in \{1,\dots,m\}} \left\{ J(\boldsymbol{x} - t\boldsymbol{v}_i) + tH^*(\boldsymbol{v}_i) \right\} \ge \inf_{\boldsymbol{v} \in \mathbb{R}^n} \left\{ J(\boldsymbol{x} - t\boldsymbol{v}) + tH^*(\boldsymbol{v}) \right\} = S_{LO}(\boldsymbol{x},t).$$

Therefore, we conclude that $f_2(\mathbf{x}, t) = S_{LO}(\mathbf{x}, t)$ for each $\mathbf{x} \in \mathbb{R}^n$ and t > 0.

Note that H is a convex function, since it is the maximum of affine functions. Then, by the same proof as in [116, Sec. 10.3.4, Thm. 3], we conclude that f_2 is a viscosity solution to the corresponding HJ PDE. Moreover, since \tilde{J} is concave, f_2 is the minimum of concave functions, which implies the concavity of f_2 . \square

Remark 3.3. In the second architecture, if we furthermore assume that the initial condition $J = \tilde{J}$ is uniformly Lipschitz, then f_2 is the unique uniformly continuous viscosity solution to the corresponding HJ PDE. This conclusion directly follows from [19, Thm. 2.1].

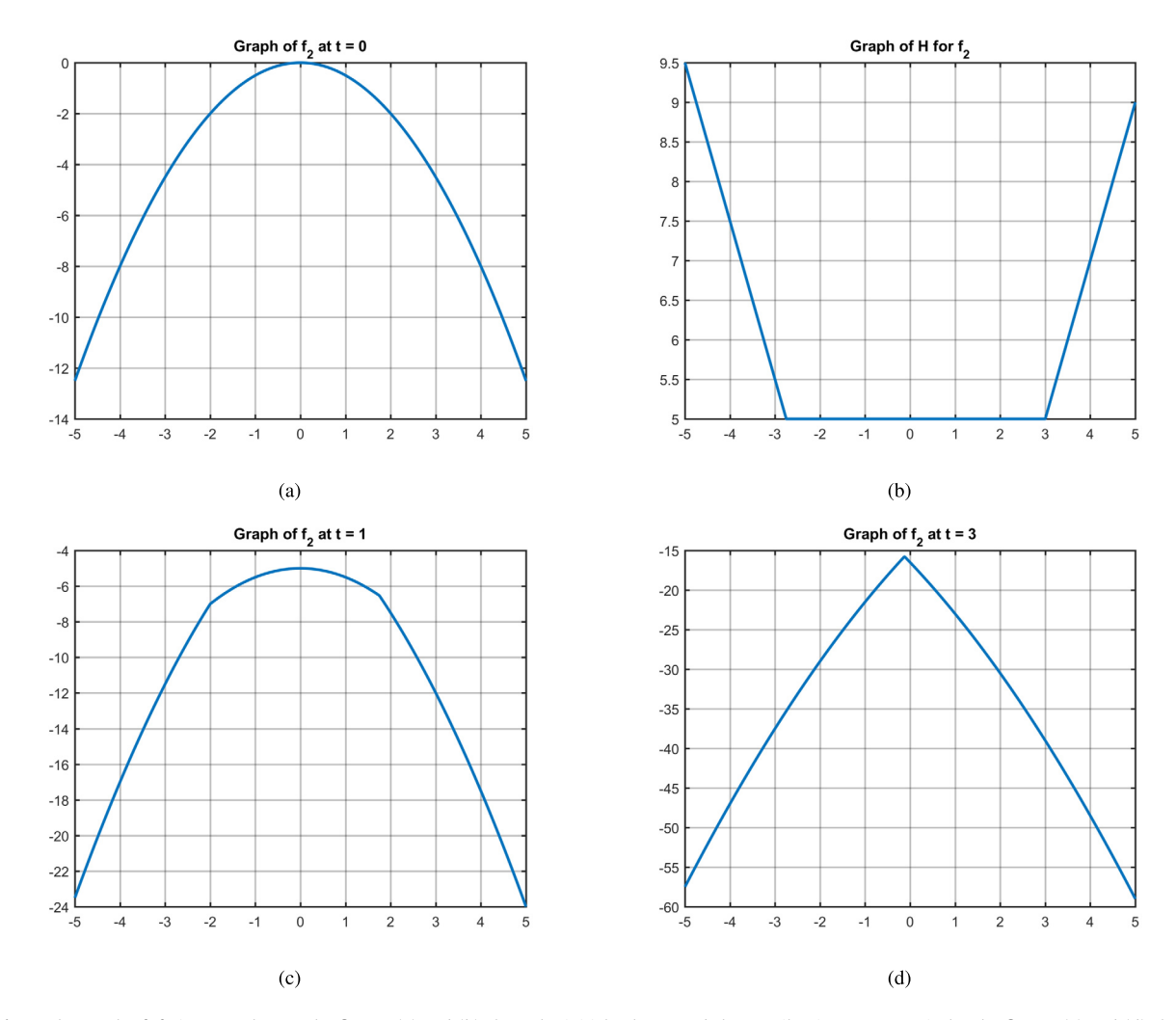


Fig. 5. The graph of f_2 in Example 3.3. The figures (a) and (b) show the initial value f_2 and the Hamiltonian f_2 , respectively. The figures (c) and (d) show the solution f_2 evaluated at f_2 and f_3 evaluated at f_4 and f_4 and f_4 and f_5 evaluated at f_4 and f_5 evaluated at f_5 eva

Example 3.3. Here, we provide a one dimensional example of the function f_2 . To be specific, we consider $f_2 : \mathbb{R} \times [0, +\infty) \to \mathbb{R}$ represented by the neural network in Fig. 2 with three neurons, i.e., we set n=1 and m=3. The initial value is given by $J(x) = -\frac{x^2}{2}$ for each $x \in \mathbb{R}$, and the Hamiltonian H is given by the piecewise affine function in Eq. (12) with $(v_1, b_1) = (-2, 0.5)$, $(v_2, b_2) = (0, -5)$ and $(v_3, b_3) = (2, 1)$. The functions J, H and H are shown in Fig. 5, where (a) shows the initial value H, (b) shows the convex Hamiltonian H, and (c) and (d) show the solution H and H and H and H are spectively. One can observe that there are several kinks on the graph of the solution shown in Fig. 2 (c) and (d), which implies that the solution given by the proposed neural network architecture is not differentiable at these kinks. In other words, the proposed architecture provides the viscosity solution to the HJ PDE without any numerical smoothing effect.

Example 3.4. Here, we present a high dimensional example. We choose the dimension to be n=10. We consider the solution $f_2: \mathbb{R}^{10} \times [0,+\infty) \to \mathbb{R}$ represented by the neural network in Fig. 2 with three neurons, i.e., we set m=3. Similar to the one dimensional case, the activation function \tilde{J} is chosen to be $\tilde{J}(\mathbf{x}) = -\frac{\|\mathbf{x}\|_2^2}{2}$ for every $\mathbf{x} \in \mathbb{R}^{10}$. Hence, by Theorem 3.2, the initial data in the corresponding HJ PDE is given by $J(\mathbf{x}) = \tilde{J}(\mathbf{x}) = -\frac{\|\mathbf{x}\|_2^2}{2}$. The parameters are chosen to be $\mathbf{v}_1 = (-2, 0, 0, 0, \dots, 0)$, $\mathbf{v}_2 = (2, -2, -1, 0, \dots, 0)$, $\mathbf{v}_3 = (0, 2, 0, 0, \dots, 0)$, $b_1 = 0.5$, $b_2 = -5$ and $b_3 = 1$. Then the Hamiltonian is the corresponding convex piecewise affine function defined in (12).

The solution f_2 is shown in Fig. 6. We fix $\mathbf{x} = (x_1, x_2, 0, \dots, 0)$ and compute $f_2(\mathbf{x}, t)$ for t = 0, 1, 3 and 5. In each figure, the color is given by the function value $f_2(\mathbf{x}, t)$ and the x and y axes represent the variables x_1 and x_2 , respectively. The solutions at t = 0, t = 1, t = 3 and t = 5 are shown in (a), (b), (c) and (d), respectively. Again, we observe kinks on the

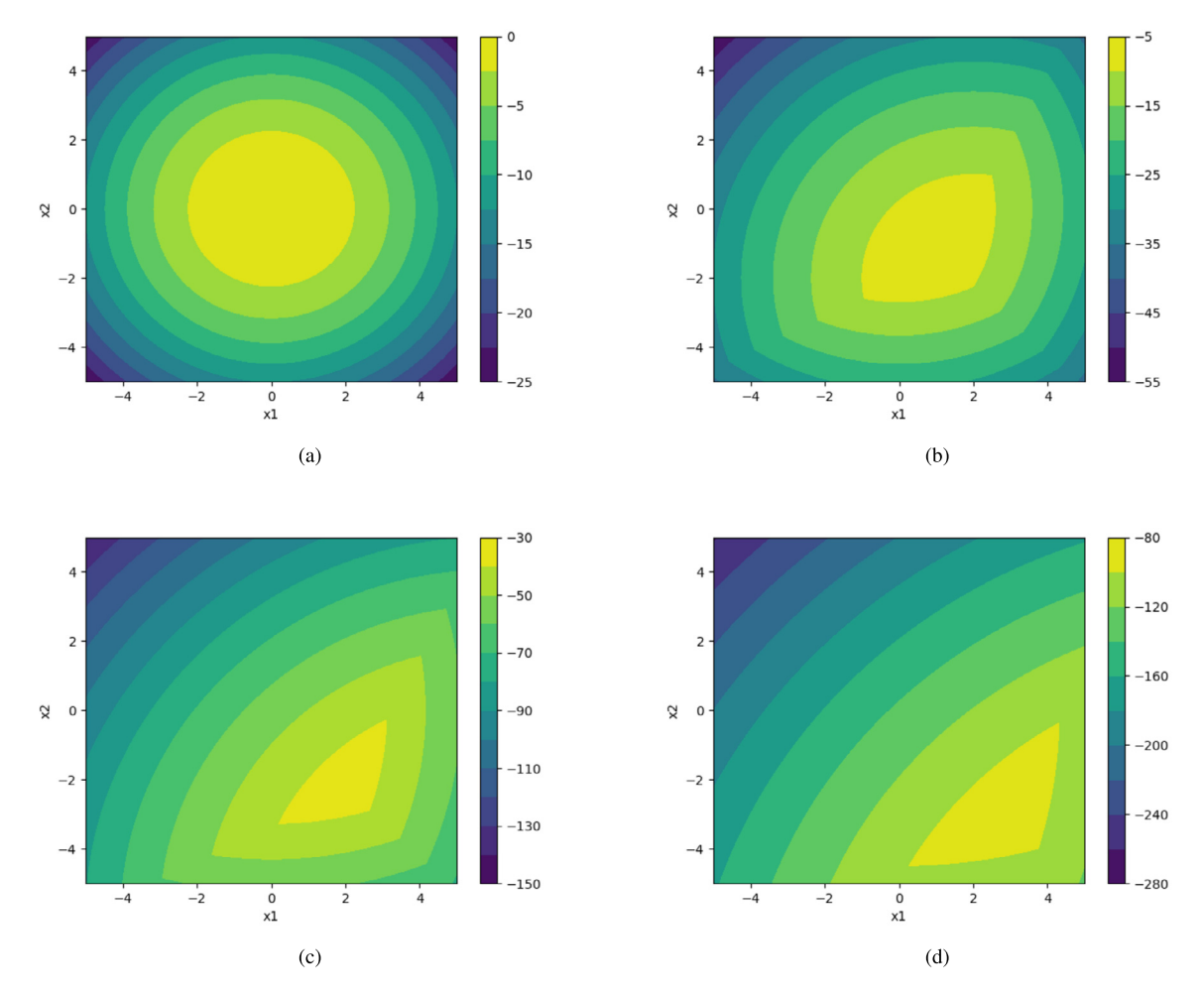


Fig. 6. A two dimensional slice of the graph of f_2 in Example 3.4. In each figure, the x and y axes correspond to the variables x_1 and x_2 , which are the first and second coordinates of the variable $\mathbf{x} = (x_1, x_2, 0, \dots, 0)$. The color is given by the function value $f_2(\mathbf{x}, t)$. The figures (a), (b), (c) and (d) show contour lines of the solution $f_2(\mathbf{x}, t)$ at t = 0, t = 1, t = 3 and t = 5, respectively.

level curves in Fig. 6 (b-d). Therefore, the proposed neural network architecture computes the viscosity solution without numerical smoothing effect.

Example 3.5. In this example, we consider two HJ PDEs defined for $\mathbf{x} \in \mathbb{R}^5$, i.e., the dimension is n=5. The initial data J is given by $J(\mathbf{x}) = -\frac{\|\mathbf{x}\|_2^2}{2}$ for each $\mathbf{x} \in \mathbb{R}^5$ and the Hamiltonian H is the l^1 -norm or the l^∞ -norm. The corresponding solutions f_2 are shown in Figs. 7 and 8. Similarly as in Example 3.4, we consider the variable $\mathbf{x} = (x_1, x_2, 0, 0, 0)$ and show the 2-dimensional slice in each figure. The solutions at t=0, t=1, t=3 and t=5 are shown in (a), (b), (c) and (d), respectively, in each figure.

When H is the l^1 -norm, i.e., $H(\mathbf{p}) = \|\mathbf{p}\|_1$ for each $\mathbf{p} \in \mathbb{R}^5$, the Hamiltonian H can be written in the form of Eq. (12) with $m = 2^n$, $b_i = 0$ for each $i \in \{1, ..., m\}$ and

$$\{\mathbf{v}_i\}_{i=1}^m = \{(w_1, w_2, \dots, w_n) \in \mathbb{R}^n : w_j \in \{\pm 1\} \, \forall j \in \{1, \dots, n\}\}.$$

The corresponding function f_2 is shown in Fig. 7.

When H is the l^{∞} -norm, i.e., $H(\mathbf{p}) = \|\mathbf{p}\|_{\infty}$ for each $\mathbf{p} \in \mathbb{R}^5$, the Hamiltonian H can be written in the form of Eq. (12) with m = 2n, $b_i = 0$ for each $i \in \{1, ..., m\}$ and

$$\{\boldsymbol{v}_i\}_{i=1}^m = \{\pm \boldsymbol{e}_j\}_{j=1}^n,$$

where e_j is the j-th coordinate basis vector in \mathbb{R}^n . The corresponding function f_2 is shown in Fig. 8.

We observe kinks on the level curves in Fig. 7 (b-d) and Fig. 8 (b-d). These numerical examples show that the proposed neural network architecture computes the viscosity solution to the HJ PDEs without any numerical smoothing effect.

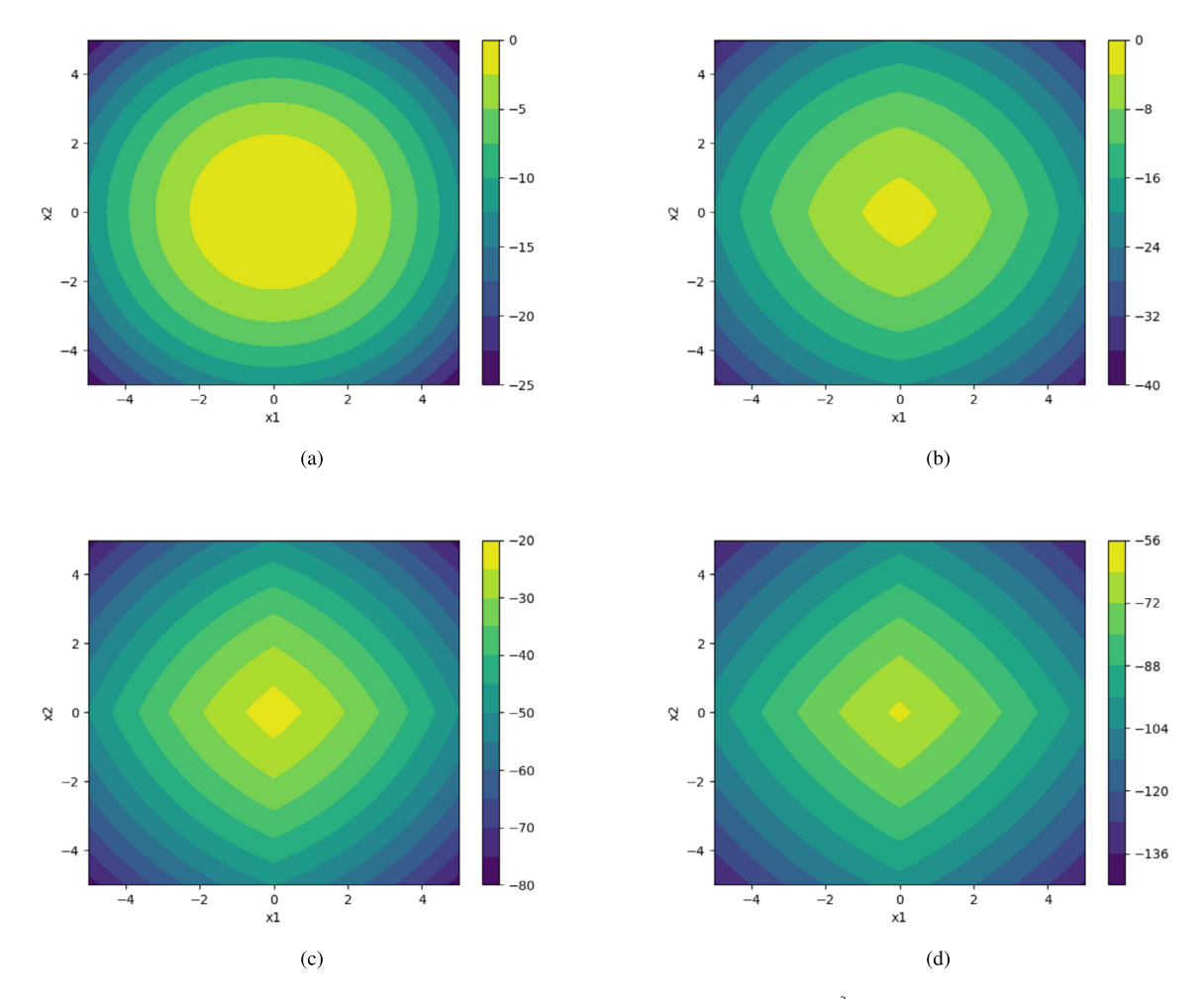


Fig. 7. A two dimensional slice of the graph of f_2 in Example 3.5. The initial data J is given by $J(\mathbf{x}) = -\frac{\|\mathbf{x}\|_2^2}{2}$ and the Hamiltonian H is the l^1 norm. In each figure, the \mathbf{x} and \mathbf{y} axes correspond to the variables \mathbf{x}_1 and \mathbf{x}_2 , which are the first and second coordinates of the variable $\mathbf{x} = (x_1, x_2, 0, \dots, 0)$. The color is given by the function value $f_2(\mathbf{x}, t)$. The figures (a), (b), (c) and (d) show contour lines of the solution $f_2(\mathbf{x}, t)$ at t = 0, t = 1, t = 3 and t = 5, respectively.

4. Conclusion

In this paper, we investigated two neural network architectures shown in Figs. 1 and 2, and proved that these two architectures represent viscosity solutions to two sets of HJ PDEs whose convex Hamiltonian H and initial data J satisfy certain assumptions in Theorems 3.1 and 3.2, respectively. This connection provides a possible interpretation for some neural network architectures. Our results suggest that efficient dedicated hardware implementation for neural networks can be leveraged to compute viscosity solutions of certain HJ PDEs. A future direction consists of implementing these neural networks on FPGA using Xilinx tools (e.g., Xilinx Vitis High Level Synthesis) to evaluate the performance of these FPGA implementations.

In this paper, we only consider the HJ PDEs whose Hamiltonian H does not depend on the state variable \boldsymbol{x} and the time variable t. Out results suggest further research directions: what kind of neural network architectures can be used to represent the viscosity solution to certain HJ PDEs whose Hamiltonian depends on \boldsymbol{x} or t? Note that a generalized Hopf-Lax formula for certain HJ PDEs with state dependent Hamiltonians is proposed in [118]. However, this formula involves a distance function which is a solution to the Eikonal equation. Hence, it is not straightforward to design a neural network architecture using this representation formula. We propose to investigate novel representation formulas for these HJ PDEs that can be represented using neural networks.

CRediT authorship contribution statement

Jérôme Darbon: Conceptualization, Methodology, Validation, Writing - original draft, Writing - review & editing. **Tingwei Meng:** Conceptualization, Methodology, Software, Validation, Writing - original draft, Writing - review & editing.

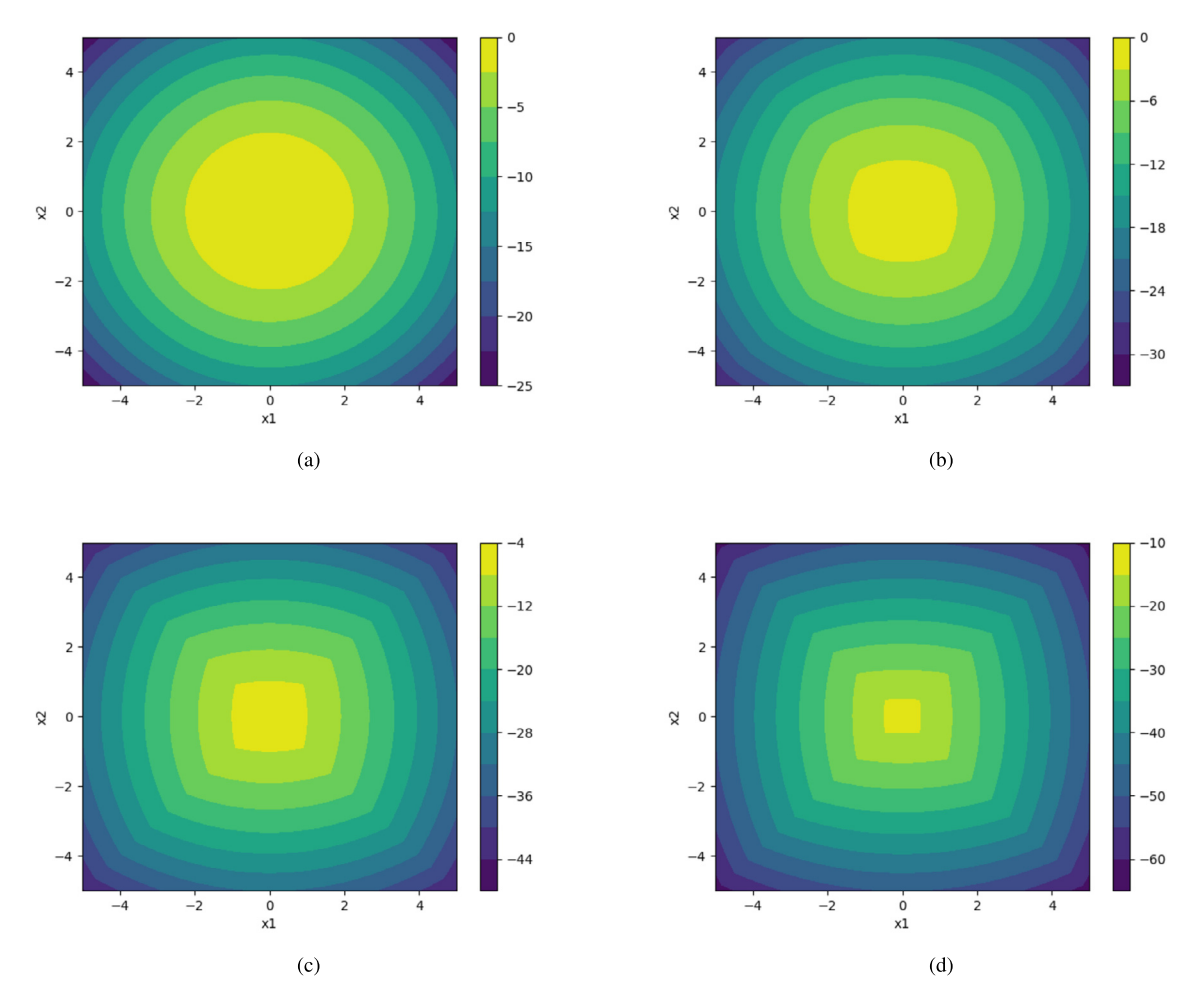


Fig. 8. A two dimensional slice of the graph of f_2 in Example 3.5. The initial data J is given by $J(\mathbf{x}) = -\frac{\|\mathbf{x}\|_2^2}{2}$ and the Hamiltonian H is the l^{∞} norm. In each figure, the x and y axes correspond to the variables x_1 and x_2 , which are the first and second coordinates of the variable $\mathbf{x} = (x_1, x_2, 0, \dots, 0)$. The color is given by the function value $f_2(\mathbf{x}, t)$. The figures (a), (b), (c) and (d) show contour lines of the solution $f_2(\mathbf{x}, t)$ at t = 0, t = 1, t = 3 and t = 5, respectively.

Declaration of competing interest

The authors declare that they have no known competing financial interests or personal relationships that could have appeared to influence the work reported in this paper.

Acknowledgements

This research is supported by NSF DMS 1820821 and AFOSR MURI FA9550-20-1-0358.

References

- [1] V.I. Arnol'd, Mathematical Methods of Classical Mechanics, Graduate Texts in Mathematics, vol. 60, Springer-Verlag, New York, 1989, Translated from the 1974 Russian original by K. Vogtmann and A. Weinstein, Corrected reprint of the second (1989) edition.
- [2] C. Carathéodory, Calculus of Variations and Partial Differential Equations of the First Order. Part I: Partial Differential Equations of the First Order, Holden-Day, Inc., San Francisco-London-Amsterdam, 1965, translated by Robert B. Dean and Julius J. Brandstatter.
- [3] C. Carathéodory, Calculus of Variations and Partial Differential Equations of the First Order. Part II: Calculus of Variations, Holden-Day, Inc., San Francisco-London-Amsterdam, 1967, Translated from the German by Robert B. Dean, Julius J. Brandstatter, translating editor.
- [4] R. Courant, D. Hilbert, Methods of Mathematical Physics, vol. II, Wiley Classics Library, John Wiley & Sons, Inc., New York, 1989, Partial differential equations, reprint of the 1962 original, a Wiley-Interscience Publication.
- [5] L. Landau, E. Lifschic, Course of Theoretical Physics, vol. 1, Mechanics, Oxford, 1978.
- [6] M. Bardi, I. Capuzzo-Dolcetta, Optimal Control and Viscosity Solutions of Hamilton-Jacobi-Bellman Equations, Systems & Control: Foundations & Applications, Birkhäuser Boston, Inc., Boston, MA, 1997, with appendices by Maurizio Falcone and Pierpaolo Soravia.
- [7] R.J. Elliott, Viscosity Solutions and Optimal Control, Pitman Research Notes in Mathematics Series, vol. 165, Longman Scientific & Technical, John Wiley & Sons, Inc., Harlow, New York, 1987.

- [8] W.H. Fleming, R.W. Rishel, Deterministic and stochastic optimal control, Bull. Am. Math. Soc. 82 (1976) 869-870.
- [9] W.H. Fleming, H.M. Soner, Controlled Markov Processes and Viscosity Solutions, vol. 25, Springer Science & Business Media, 2006.
- [10] W. McEneaney, Max-Plus Methods for Nonlinear Control and Estimation, Springer Science & Business Media, 2006.
- [11] E. Barron, L. Evans, R. Jensen, Viscosity solutions of Isaacs' equations and differential games with Lipschitz controls, J. Differ. Equ. 53 (1984) 213–233.
- [12] R. Buckdahn, P. Cardaliaguet, M. Quincampoix, Some recent aspects of differential game theory, Dyn. Games Appl. 1 (2011) 74-114.
- [13] L.C. Evans, P.E. Souganidis, Differential games and representation formulas for solutions of Hamilton-Jacobi-Isaacs equations, Indiana Univ. Math. J. 33 (1984) 773–797.
- [14] H. Ishii, Representation of solutions of Hamilton-Jacobi equations, Nonlinear Anal., Theory Methods Appl. 12 (1988) 121-146.
- [15] J. Darbon, On convex finite-dimensional variational methods in imaging sciences and Hamilton–Jacobi equations, SIAM J. Imaging Sci. 8 (2015) 2268–2293.
- [16] J. Darbon, T. Meng, On decomposition models in imaging sciences and multi-time Hamilton–Jacobi partial differential equations, SIAM J. Imaging Sci. 13 (2020) 971–1014.
- [17] J. Darbon, S. Osher, Algorithms for overcoming the curse of dimensionality for certain Hamilton–Jacobi equations arising in control theory and elsewhere, Res. Math. Sci. 3 (2016) 19.
- [18] J. Darbon, G.P. Langlois, T. Meng, Overcoming the curse of dimensionality for some Hamilton-Jacobi partial differential equations via neural network architectures, Res. Math. Sci. 7 (2020) 20.
- [19] M. Bardi, L. Evans, On Hopf's formulas for solutions of Hamilton-Jacobi equations, Nonlinear Anal., Theory Methods Appl. 8 (1984) 1373-1381.
- [20] G. Barles, Solutions de viscosité des équations de Hamilton-Jacobi, Mathématiques et Applications, Springer-Verlag, Berlin, Heidelberg, 1994.
- [21] M.G. Crandall, H. Ishii, P.-L. Lions, User's guide to viscosity solutions of second order partial differential equations, Bull. Am. Math. Soc. 27 (1992) 1–67.
- [22] Y. LeCun, Deep learning hardware: past, present, and future, in: 2019 IEEE International Solid-State Circuits Conference (ISSCC), 2019, pp. 12-19.
- [23] C. Farabet, Y. LeCun, K. Kavukcuoglu, E. Culurciello, B. Martini, P. Akselrod, S. Talay, Large-scale fpga-based convolutional networks, in: R. Bekkerman, M. Bilenko, J. Langford (Eds.), Scaling up Machine Learning: Parallel and Distributed Approaches, Cambridge University Press, 2011.
- [24] C. Farabet, C. poulet, J. Han, Y. LeCun, Cnp: an fpga-based processor for convolutional networks, in: International Conference on Field Programmable Logic and Applications, IEEE, Prague, 2009.
- [25] C. Farabet, C. Poulet, Y. LeCun, An fpga-based stream processor for embedded real-time vision with convolutional networks, in: 2009 IEEE 12th International Conference on Computer Vision Workshops, ICCV Workshops, IEEE Computer Society, Los Alamitos, CA, USA, 2009, pp. 878–885, https://doi.ieeecomputersociety.org/10.1109/ICCVW.2009.5457611.
- [26] K. Banerjee, E. Georganas, D. Kalamkar, B. Ziv, E. Segal, C. Anderson, A. Heinecke, Optimizing deep learning rnn topologies on intel architecture, Supercomput. Frontiers Innovat. 6 (2019).
- [27] N.P. Jouppi, C. Young, N. Patil, D. Patterson, G. Agrawal, R. Bajwa, S. Bates, S. Bhatia, N. Boden, A. Borchers, et al., In-datacenter performance analysis of a tensor processing unit, in: Proceedings of the 44th Annual International Symposium on Computer Architecture, ISCA'17, Association for Computing Machinery, New York, NY, USA, 2017, pp. 1–12.
- [28] A. Kundu, S. Srinivasan, E.C. Qin, D. Kalamkar, N.K. Mellempudi, D. Das, K. Banerjee, B. Kaul, P. Dubey, K-tanh: hardware efficient activations for deep learning, arXiv preprint arXiv:1909.07729, 2019.
- [29] T. Chen, J. van Gelder, B. van de Ven, S.V. Amitonov, B. de Wilde, H.-C.R. Euler, H. Broersma, P.A. Bobbert, F.A. Zwanenburg, W.G. van der Wiel, Classification with a disordered dopant-atom network in silicon, Nature 577 (2020) 341–345.
- [30] C. Hirjibehedin, Evolution of circuits for machine learning, Nature 577 (2020) 320–321.
- [31] M. Akian, R. Bapat, S. Gaubert, Max-plus algebra, in: Handbook of Linear Algebra, vol. 39, 2006.
- [32] M. Akian, S. Gaubert, A. Lakhoua, The max-plus finite element method for solving deterministic optimal control problems: basic properties and convergence analysis, SIAM J. Control Optim. 47 (2008) 817–848.
- [33] P.M. Dower, W.M. McEneaney, H. Zhang, Max-plus fundamental solution semigroups for optimal control problems, in: 2015 Proceedings of the Conference on Control and Its Applications, SIAM, 2015, pp. 368–375.
- [34] W. Fleming, W. McEneaney, A max-plus-based algorithm for a Hamilton-Jacobi-Bellman equation of nonlinear filtering, SIAM J. Control Optim. 38 (2000) 683-710.
- [35] S. Gaubert, W. McEneaney, Z. Qu, Curse of dimensionality reduction in max-plus based approximation methods: theoretical estimates and improved pruning algorithms, in: 2011 50th IEEE Conference on Decision and Control and European Control Conference, IEEE, 2011, pp. 1054–1061.
- [36] W. McEneaney, A curse-of-dimensionality-free numerical method for solution of certain HJB PDEs, SIAM J. Control Optim. 46 (2007) 1239-1276.
- [37] W.M. McEneaney, A. Deshpande, S. Gaubert, Curse-of-complexity attenuation in the curse-of-dimensionality-free method for HJB PDEs, in: 2008 American Control Conference, IEEE, 2008, pp. 4684–4690.
- [38] W.M. McEneaney, L.J. Kluberg, Convergence rate for a curse-of-dimensionality-free method for a class of HJB PDEs, SIAM J. Control Optim. 48 (2009) 3052–3079.
- [39] A. Alla, M. Falcone, L. Saluzzi, An efficient DP algorithm on a tree-structure for finite horizon optimal control problems, SIAM J. Sci. Comput. 41 (2019) A2384–A2406.
- [40] D.P. Bertsekas, Reinforcement Learning and Optimal Control, Athena Scientific, Belmont, Massachusetts, 2019.
- [41] S. Dolgov, D. Kalise, K. Kunisch, A tensor decomposition approach for high-dimensional Hamilton-Jacobi-Bellman equations, arXiv preprint: arXiv: 1908.01533, 2019.
- [42] M.B. Horowitz, A. Damle, J.W. Burdick, Linear Hamilton Jacobi Bellman equations in high dimensions, in: 53rd IEEE Conference on Decision and Control, IEEE, 2014, pp. 5880–5887.
- [43] E. Todorov, Efficient computation of optimal actions, Proc. Natl. Acad. Sci. 106 (2009) 11478–11483.
- [44] O. Bokanowski, J. Garcke, M. Griebel, I. Klompmaker, An adaptive sparse grid semi-Lagrangian scheme for first order Hamilton-Jacobi Bellman equations, J. Sci. Comput. 55 (2013) 575–605.
- [45] J. Garcke, A. Kröner, Suboptimal feedback control of PDEs by solving HJB equations on adaptive sparse grids, J. Sci. Comput. 70 (2017) 1-28.
- [46] W. Kang, L.C. Wilcox, Mitigating the curse of dimensionality: sparse grid characteristics method for optimal feedback control and HJB equations, Comput. Optim. Appl. 68 (2017) 289–315.
- [47] A. Alla, M. Falcone, S. Volkwein, Error analysis for POD approximations of infinite horizon problems via the dynamic programming approach, SIAM J. Control Optim. 55 (2017) 3091–3115.
- [48] K. Kunisch, S. Volkwein, L. Xie, HJB-POD-based feedback design for the optimal control of evolution problems, SIAM J. Appl. Dyn. Syst. 3 (2004) 701–722.
- [49] D. Kalise, S. Kundu, K. Kunisch, Robust feedback control of nonlinear PDEs by numerical approximation of high-dimensional Hamilton-Jacobi-Isaacs equations, arXiv preprint: arXiv:1905.06276, 2019.
- [50] D. Kalise, K. Kunisch, Polynomial approximation of high-dimensional Hamilton–Jacobi–Bellman equations and applications to feedback control of semilinear parabolic PDEs, SIAM J. Sci. Comput. 40 (2018) A629–A652.
- [51] I. Yegorov, P.M. Dower, Perspectives on characteristics based curse-of-dimensionality-free numerical approaches for solving Hamilton–Jacobi equations, Appl. Math. Optim. (2017) 1–49.

- [52] A. Bachouch, C. Huré, N. Langrené, H. Pham, Deep neural networks algorithms for stochastic control problems on finite horizon: numerical applications, arXiv preprint: arXiv:1812.05916, 2018.
- [53] B. Djeridane, J. Lygeros, Neural approximation of PDE solutions: an application to reachability computations, in: Proceedings of the 45th IEEE Conference on Decision and Control, 2006, pp. 3034–3039.
- [54] F. Jiang, G. Chou, M. Chen, C.J. Tomlin, Using neural networks to compute approximate and guaranteed feasible Hamilton-Jacobi-Bellman PDE solutions, arXiv preprint: arXiv:1611.03158, 2016.
- [55] J. Han, A. Jentzen, W. E, Solving high-dimensional partial differential equations using deep learning, Proc. Natl. Acad. Sci. 115 (2018) 8505-8510.
- [56] C. Huré, H. Pham, A. Bachouch, N. Langrené, Deep neural networks algorithms for stochastic control problems on finite horizon, part I: convergence analysis, arXiv preprint: arXiv:1812.04300, 2018.
- [57] C. Huré, H. Pham, X. Warin, Some machine learning schemes for high-dimensional nonlinear PDEs, arXiv preprint: arXiv:1902.01599, 2019.
- [58] P. Lambrianides, Q. Gong, D. Venturi, A new scalable algorithm for computational optimal control under uncertainty, arXiv preprint: arXiv:1909.07960, 2019.
- [59] K.N. Niarchos, J. Lygeros, A neural approximation to continuous time reachability computations, in: Proceedings of the 45th IEEE Conference on Decision and Control, 2006, pp. 6313–6318.
- [60] C. Reisinger, Y. Zhang, Rectified deep neural networks overcome the curse of dimensionality for nonsmooth value functions in zero-sum games of nonlinear stiff systems, arXiv preprint: arXiv:1903.06652, 2019.
- [61] V.R. Royo, C. Tomlin, Recursive regression with neural networks: approximating the HJI PDE solution, arXiv preprint: arXiv:1611.02739, 2016.
- [62] J. Sirignano, K. Spiliopoulos, DGM: a deep learning algorithm for solving partial differential equations, J. Comput. Phys. 375 (2018) 1339-1364.
- [63] C. Beck, S. Becker, P. Grohs, N. Jaafari, A. Jentzen, Solving stochastic differential equations and Kolmogorov equations by means of deep learning, arXiv preprint: arXiv:1806.00421, 2018.
- [64] C. Beck, S. Becker, P. Cheridito, A. Jentzen, A. Neufeld, Deep splitting method for parabolic PDEs, arXiv preprint: arXiv:1907.03452.
- [65] C. Beck, E. Weinan, A. Jentzen, Machine learning approximation algorithms for high-dimensional fully nonlinear partial differential equations and second-order backward stochastic differential equations, J. Nonlinear Sci. 29 (2019) 1563–1619.
- [66] J. Berg, K. Nyström, A unified deep artificial neural network approach to partial differential equations in complex geometries, Neurocomputing 317 (2018) 28–41.
- [67] O. Chan-Wai-Nam, J. Mikael, X. Warin, Machine learning for semi linear PDEs, J. Sci. Comput. 79 (2019) 1667-1712.
- [68] T. Cheng, F.L. Lewis, Fixed-final time constrained optimal control of nonlinear systems using neural network HJB approach, in: Proceedings of the 45th IEEE Conference on Decision and Control, 2006, pp. 3016–3021.
- [69] M.W.M.G. Dissanayake, N. Phan-Thien, Neural-network-based approximations for solving partial differential equations, Commun. Numer. Methods Eng. 10 (1994) 195–201.
- [70] T. Dockhorn, A discussion on solving partial differential equations using neural networks, arXiv preprint: arXiv:1904.07200, 2019.
- [71] W. E, J. Han, A. Jentzen, Deep learning-based numerical methods for high-dimensional parabolic partial differential equations and backward stochastic differential equations, Commun. Math. Stat. 5 (2017) 349–380.
- [72] A.B. Farimani, J. Gomes, V.S. Pande, Deep learnin the physics of transport phenomena, 2017, arXiv:e-prints.
- [73] M. Fujii, A. Takahashi, M. Takahashi, Asymptotic expansion as prior knowledge in deep learning method for high dimensional BSDEs, Asia-Pac. Financ. Mark. 26 (2019) 391–408.
- [74] P. Grohs, A. Jentzen, D. Salimova, Deep neural network approximations for Monte Carlo algorithms, arXiv preprint; arXiv:1908.10828, 2019.
- [75] J. Han, L. Zhang, E. Weinan, Solving many-electron Schrödinger equation using deep neural networks, J. Comput. Phys. (2019) 108929.
- [76] J.-T. Hsieh, S. Zhao, S. Eismann, L. Mirabella, S. Ermon, Learning neural PDE solvers with convergence guarantees, in: International Conference on Learning Representations, 2019.
- [77] L. Jianyu, L. Siwei, Q. Yingjian, H. Yaping, Numerical solution of elliptic partial differential equation using radial basis function neural networks, Neural Netw. 16 (2003) 729–734.
- [78] Y. Khoo, J. Lu, L. Ying, Solving parametric PDE problems with artificial neural networks, arXiv preprint: arXiv:1707.03351, 2017.
- [79] Y. Khoo, J. Lu, L. Ying, Solving for high-dimensional committor functions using artificial neural networks, Res. Math. Sci. 6 (2019) 1.
- [80] I.E. Lagaris, A. Likas, D.I. Fotiadis, Artificial neural networks for solving ordinary and partial differential equations, IEEE Trans. Neural Netw. 9 (1998) 987–1000
- [81] I.E. Lagaris, A.C. Likas, D.G. Papageorgiou, Neural-network methods for boundary value problems with irregular boundaries, IEEE Trans. Neural Netw. 11 (2000) 1041–1049.
- [82] H. Lee, I.S. Kang, Neural algorithm for solving differential equations, J. Comput. Phys. 91 (1990) 110-131.
- [83] K.O. Lye, S. Mishra, D. Ray, Deep learning observables in computational fluid dynamics, arXiv preprint: arXiv:1903.03040, 2019.
- [84] K.S. McFall, J.R. Mahan, Artificial neural network method for solution of boundary value problems with exact satisfaction of arbitrary boundary conditions, IEEE Trans. Neural Netw. 20 (2009) 1221–1233.
- [85] A. Meade, A. Fernandez, The numerical solution of linear ordinary differential equations by feedforward neural networks, Math. Comput. Model. 19 (1994) 1–25.
- [86] B.P. van Milligen, V. Tribaldos, J.A. Jiménez, Neural network differential equation and plasma equilibrium solver, Phys. Rev. Lett. 75 (1995) 3594-3597.
- [87] H. Pham, H. Pham, X. Warin, Neural networks-based backward scheme for fully nonlinear PDEs, arXiv preprint; arXiv:1908.00412, 2019.
- [88] K. Rudd, G.D. Muro, S. Ferrari, A constrained backpropagation approach for the adaptive solution of partial differential equations, IEEE Trans. Neural Netw. Learn. Syst. 25 (2014) 571–584.
- [89] W. Tang, T. Shan, X. Dang, M. Li, F. Yang, S. Xu, J. Wu, Study on a Poisson's equation solver based on deep learning technique, in: 2017 IEEE Electrical Design of Advanced Packaging and Systems Symposium (EDAPS), 2017, pp. 1–3.
- [90] Y. Tassa, T. Erez, Least squares solutions of the HJB equation with neural network value-function approximators, IEEE Trans. Neural Netw. 18 (2007) 1031–1041.
- [91] E. Weinan, B. Yu, The deep Ritz method: a deep learning-based numerical algorithm for solving variational problems, Commun. Math. Stat. 6 (2018) 1–12.
- [92] N. Yadav, A. Yadav, M. Kumar, An Introduction to Neural Network Methods for Differential Equations, SpringerBriefs in Applied Sciences and Technology, Springer, Dordrecht, 2015.
- [93] L. Yang, D. Zhang, G.E. Karniadakis, Physics-informed generative adversarial networks for stochastic differential equations, arXiv preprint: arXiv: 1811.02033, 2018.
- [94] Y. Yang, P. Perdikaris, Adversarial uncertainty quantification in physics-informed neural networks, J. Comput. Phys. 394 (2019) 136-152.
- [95] W. Zhao, T. Zhou, T. Kong, High order numerical schemes for second-order FBSDEs with applications to stochastic optimal control, Commun. Comput. Phys. 21 (2017) 808–834.
- [96] T. Kong, W. Zhao, T. Zhou, Probabilistic high order numerical schemes for fully nonlinear parabolic PDEs, Commun. Comput. Phys. 18 (2015) 1482–1503.
- [97] Z. Long, Y. Lu, X. Ma, B. Dong, PDE-net: learning PDEs from data, arXiv:1710.09668, 2017.

- [98] Z. Long, Y. Lu, B. Dong, PDE-net 2.0: learning PDEs from data with a numeric-symbolic hybrid deep network, J. Comput. Phys. 399 (2019) 108925.
- [99] X. Meng, G.E. Karniadakis, A composite neural network that learns from multi-fidelity data: application to function approximation and inverse PDE problems, arXiv preprint: arXiv:1903.00104, 2019.
- [100] X. Meng, Z. Li, D. Zhang, G.E. Karniadakis, PPINN: parareal physics-informed neural network for time-dependent PDEs, arXiv preprint: arXiv:1909. 10145, 2019.
- [101] G. Pang, L. Lu, G.E. Karniadakis, fPINNs: fractional physics-informed neural networks, SIAM J. Sci. Comput. 41 (2019) A2603-A2626.
- [102] M. Raissi, Deep hidden physics models; deep learning of nonlinear partial differential equations, J. Mach. Learn. Res. 19 (2018) 932–955.
- [103] M. Raissi, Forward-backward stochastic neural networks: deep learning of high-dimensional partial differential equations, arXiv preprint: arXiv:1804. 07010.
- [104] M. Raissi, P. Perdikaris, G.E. Karniadakis, Physics informed deep learning (part I): data-driven solutions of nonlinear partial differential equations, arXiv preprint: arXiv:1711.10561.
- [105] M. Raissi, P. Perdikaris, G.E. Karniadakis, Physics informed deep learning (part ii): data-driven discovery of nonlinear partial differential equations, arXiv preprint: arXiv:1711.10566.
- [106] M. Raissi, P. Perdikaris, G. Karniadakis, Physics-informed neural networks: a deep learning framework for solving forward and inverse problems involving nonlinear partial differential equations, J. Comput. Phys. 378 (2019) 686–707.
- [107] T. Uchiyama, N. Sonehara, Solving inverse problems in nonlinear PDEs by recurrent neural networks, in: IEEE International Conference on Neural Networks, IEEE, 1993, pp. 99–102.
- [108] D. Zhang, L. Guo, G.E. Karniadakis, Learning in modal space: solving time-dependent stochastic PDEs using physics-informed neural networks, arXiv preprint: arXiv:1905.01205.
- [109] D. Zhang, L. Lu, L. Guo, G.E. Karniadakis, Quantifying total uncertainty in physics-informed neural networks for solving forward and inverse stochastic problems, J. Comput. Phys. 397 (2019) 108850.
- [110] Y. Fan, L. Ying, Solving inverse wave scattering with deep learning, arXiv preprint: arXiv:1911.13202, 2019.
- [111] L. Yan, T. Zhou, An adaptive surrogate modeling based on deep neural networks for large-scale Bayesian inverse problems, arXiv preprint: arXiv: 1911.08926, 2019.
- [112] L.Á.L. Cárdenas, F. Gibou, A deep learning approach for the computation of curvature in the level-set method, arXiv preprint: arXiv:2002.02804, 2020.
- [113] J.-B. Hiriart-Urruty, C. Lemaréchal, Convex Analysis and Minimization Algorithms I: Fundamentals, vol. 305, Springer Science & Business Media, 1993.
- [114] J.-B. Hiriart-Urruty, C. Lemaréchal, Convex Analysis and Minimization Algorithms II: Advanced Theory and Bundle Methods, vol. 306, Springer Science & Business Media, 1993.
- [115] R.T. Rockafellar, Convex Analysis, Princeton University Press, 1970.
- [116] L.C. Evans, Partial Differential Equations, second ed., Graduate Studies in Mathematics, vol. 19, American Mathematical Society, Providence, RI, 2010.
- [117] E. Hopf, Generalized solutions of non-linear equations of first order, J. Math. Mech. 14 (1965) 951-973.
- [118] F. Dragoni, Metric Hopf-Lax formula with semicontinuous data, Discrete Contin. Dyn. Syst. 17 (2007) 713-729.